Modelling of Ion-Diamagnetic Effects on Ideal MHD Modes in Tokamak Plasmas

G.T.A. Huysmans, S.E. Sharapov[1], A.B. Mikhailovskii[2]
Association Euratom-CEA Cadarache, 13108 St-Paul-lez-Durance, France
[1]JET, Abingdon, OX14 3EA, United Kingdom
[2]Institute for Nuclear Fusion, RRC Kurchatov Institute, Kurchatov Sqr. 1, Moscow Russia

Introduction

Ideal MHD instabilities are an important factor in the limitation of the plasma performance (fusion yield) in many devices. Generally, these instabilities are related to the large pressure gradients in the transport barriers which are characteristic for the high performance discharges, either at the plasma edge in the H-mode or at about mid radius in the case of Optimised Shear discharges. The large ion-diamagnetic drift velocity due to the pressure gradients has usually been ignored in the MHD stability calculations. It is, however, well known that ion-diamagnetic drift (ω_i*) can have a significant stabilising effect on MHD instabilities. In order to study the effect of a finite drift velocity on the ideal MHD modes, the linear ideal MHD code MISHKA-1 [1] has been extended to include the effects of a finite ion diamagnetic drift velocity. In this paper, the influence of the ion-diamagnetic drift is analysed for the localised kink and ballooning modes in the H-mode edge pedestal and for the global modes in optimised shear scenarios with internal transport barriers.

The Model

The ion-drift velocity follows from the ion momentum equation (see [2]). Normalising the equations with respect to the equilibrium density (n_m), major radius (R_m) and vacuum magnetic field (B_m) on the magnetic axis yields for the equilibrium ion velocity (normalised to the Alfvén velocity on axis):

$$\mathbf{v}_0 = \frac{\tau}{\rho_0 B_0^2}\mathbf{B}_0 \times \nabla p_{oi} \ , \qquad \tau = \frac{1}{e_i R_m}\sqrt{\frac{m_i}{\mu_0 n_m}} = \frac{1}{\omega_{ci}\tau_A} = \frac{0.072\sqrt{A}}{R_m[m]\sqrt{n_m[10^{19}\,m^{-3}]}} \qquad (1)$$

where τ is a dimensionless quantity (the ion-cyclotron frequency normalised to the Alfvén time, τ_A) measuring the amplitude of the non-ideal MHD terms. The linearised momentum equation including the ion-drift velocity takes the form:

$$\lambda\rho_0\left(\mathbf{v} + \frac{\tau}{B_0^2}\mathbf{B}_0 \times \nabla\left(\frac{p_i'}{\rho_0}\right)\right) = -\nabla p' + (\nabla\times\mathbf{B_0})\times\mathbf{B} - \mathbf{B_0}\times(\nabla\times\mathbf{B}) \ , \qquad (2)$$

where p is the perturbed pressure $p' = p_0' A_2$, $A_2 = (\mathbf{A}\times\mathbf{B_0})_1 / B_0^2$, ρ_0 is the mass density, **B** is the magnetic field perturbation, λ is the eigenvalue normalised to the Alfvén time.

The new terms due to the equilibrium ion velocity have been added to the MISHKA-1 code. This doubles the number of variables in the new code (MISHKA-D) to 4, two for the velocity and two for the vector potential. The eigenvalues are in general complex. As with the MISHKA-1 code, both instabilities and the stable part of the spectrum can be obtained in general toroidal geometry and for arbitrary plasma shapes.

Stability limits of the edge pedestal

The pressure gradient in the edge pedestal of an H-mode discharge is limited by MHD stability, notably the ballooning limit due to high-n pressure driven modes and the kink limit due to low-n current driven kink modes (peeling modes).

Edge ballooning modes

The marginally stable values of the pressure gradient in the edge pedestal have been calculated with the MISHKA code in full toroidal geometry for toroidal mode numbers between n = 10 and n = 40 as a function of the width of the edge pedestal. The equilibrium used has a circular plasma boundary with aspect ratio 4, q at the boundary just below 4 and

β_p=1.0. The edge pedestal is represented by adding a local gradient to the pressure profile: $p'(\psi) = 1-\psi + p_1 ((\psi-\psi_b)^2 (3-2\psi-\psi_b)/(1-\psi_b)^3)^{1/4}$. The increased pressure gradient extends from ψ_b to the boundary (ψ=1). The current density profile is given by $<j> = 1-0.8\psi-0.2\psi^2$, ψ is the normalised poloidal flux. In the stability calculations an ideally conducting wall is positioned at twice the minor radius.

The *ideal* MHD marginally stable values of the pressure gradient α_c due to finite-n ballooning modes (as calculated with MISHKA-1), are well described by:

$$\alpha_c(n) = \alpha(\infty) + c_1/(\delta_b n), \qquad \alpha = -4(q^2/\varepsilon B_0^2)V^{1/2}(dp/dV) \ , \tag{3}$$

with δ_b the width of the barrier, $\delta_b = (1 - \psi_b^{1/2})$ and $\alpha(\infty)$ is the $n\rightarrow\infty$ ballooning limit. The $1/n$ correction of the critical α is consistent with the conventional ballooning mode theory. The modified scaling, $\sim n^{-2/3}$, for edge ballooning modes as found in [3] is related to the assumed linear variation of the growth rate of the $n=\infty$ ballooning mode. For the profile shapes used here, the $n=\infty$ growth rate varies quadratrically as a function of ψ, as in the conventional ballooning theory. The correction to α_c is inversely proportional to the width of the edge pedestal, i.e. narrow barriers are more stable at lower toroidal mode numbers. The width of the high-n modes in the pedestal does not follow the $1/\sqrt{n}$ dependence expected from the ballooning theory. Instead, the width (as measured by half-width of the envelope of the mode at the outboard mid-plane) shows a strong scaling with the pedestal width and a weak scaling with toroidal mode number: $\delta_{HW} \sim \delta_b^{3/4} n^{-1/4}$. The number of rational surfaces within the half-width of the mode, which scales as $\sqrt{n}$ in the ballooning theory, increases linearly with n, leading to a mode width independent of n.

Close to marginal stability, for the range of toroidal mode numbers considered (10<n<40), the growth rates of the ideal MHD high-n modes can be described by:

$$\lambda^2 = c_2 \, \mathbf{n} \, (\alpha - \alpha_c). \tag{4}$$

For larger growth rates (> 0.050), the growth rate follows the conventional ballooning scaling:

$$\lambda^2 = c_3 \, (1 - c_4/(\delta_b \, \mathbf{n})) \, (\alpha - \alpha_c) \tag{5}$$

i.e., the growth rate saturates as $n \rightarrow \infty$. (The α_c values in (3) and (4) have slightly different numerical values). The scaling of the growth rate close to marginal stability (Eq.4) is due to the free boundary contribution to the instability and depends on the precise value of q at the boundary. The behaviour for larger growth rates is relatively independent of q at the boundary.

The influence of the diamagnetic drift on the growth rates and frequencies of the ideal MHD ballooning modes has been evaluated with the MISHKA-D code. The eigenvalues of the finite-n ballooning modes follows the well-known dispersion relation:

$$\lambda(\lambda - i\omega_{*_i}) = \lambda_{ideal}^2 \ , \qquad \omega_{*_i} = \frac{\langle \nabla \psi \rangle}{\langle r \rangle \langle B_0 \rangle} \frac{nq\tau}{\rho} p_i' \ , \tag{6}$$

where the ion diamagnetic frequency ω_{*i} is a function of the minor radius. Taking the value of ω^* in the middle of the edge pedestal gives good agreement with the calculated eigenvalues. Assuming that Eq.(6) holds for all mode numbers and values of the growth rates, the marginal stability curves at finite ω^* can be determined using only the ideal MHD growth rates. The modes become stable for $\omega^* > 2\lambda_{ideal}$. From a comparison of the scaling of the ideal MHD growth rates $(\lambda \sim 1 - c_4/2n)$ and $\omega^* (= c_\omega \, \tau \, n \, \alpha)$ with the toroidal mode number it is clear that the high-n ballooning modes are most easily stabilised. With increasing τ, i.e. decreasing density, the most unstable mode number decreases and the stability limit will be determined by the medium to low-n stability limit. For large enough values of τ and n the ballooning modes will be stable for any values of α. The stability limit of the ballooning modes at finite ω^* as calculated with the MISHKA-D code are shown in Fig.1. These calculations self-consistently include the finite ion-diamagnetic drift. The resulting marginally stable values for α agree very well with the values based on the ideal MHD growth rates for τ < 0.02. For τ=0.01, the most unstable mode is n=20 and there is no stability limit for toroidal mode

numbers larger than 40. For τ=0.02, the stabilisation is less than expected from Eq. 6. This is related to the increased interaction with the Alfven continuum, which causes a significant change of the mode structure which extends well beyond the edge pedestal. The frequency of the marginally stable modes at τ=0.02 is inside the first Alfven gap (outside the edge pedestal).

Low-n kink and ballooning limits

The low-n kink (peeling modes) are driven unstable by the edge current density which consists mostly of bootstrap current due to the edge pressure gradient. Even in ideal MHD this pressure gradient is known to have a significant stabilising effect on low-n kink mode, for pressure gradients below the ballooning limit. The influence of the ion-diamagnetic drift on the stability of low-n modes, as computed with the MISHKA-D code, is shown in an edge stability diagram (see Fig.2).

At the ballooning limit the stabilising effect on the low-n kink modes is of the same order for the different mode numbers. This is because both the growth rate and the diamagnetic frequency increase linearly with mode number. (For this equilibrium the second stable regime for ideal ballooning modes exists only for $j_1/j_0 > 0.42$ and is not accessible due to the low-n stability limits.)

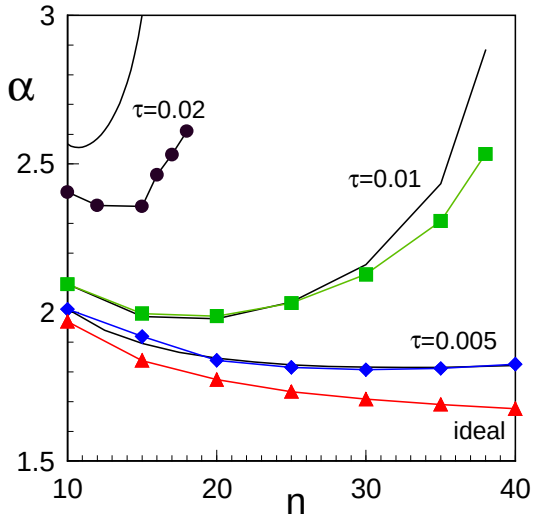

Fig.1 *Finite-n ballooning limit as a function of toroidal mode number for several value of τ (MISHKA-D). Included are the values based on ideal MHD growth rates (Eq.6).*

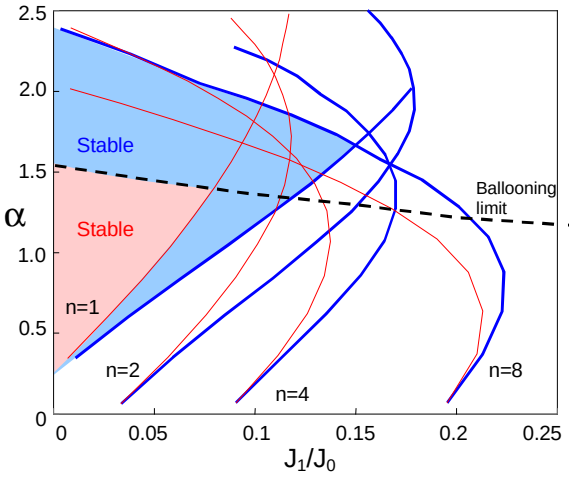

Fig.2 *The kink and ballooning stability limits as a function of the edge pressure gradient and edge current density for τ=0 (thin lines) and τ=0.02 (fat lines). Included is the n=∞ ballooning limit (dashed). The shaded areas are stable.*

JET Hot-Ion H-mode

In order to quantify the importance of the stabilising influence ion-diamagnetic drift, the stability limits due to kink and ballooning modes have been calculated for a JET hot-ion H-mode DT discharge (#42677) at the time of maximum performance. The profiles for the pressure and the current profile are taken from a transport simulation of this discharge with the JETTO code. The width of the transport barrier is ~ 4 cm. Fig.3 shows the relevant stability limits for this discharge as a function of τ. The maximum edge current density is limited by an n=2 kink (peeling) mode. The increase in the marginally stable edge current is to first order linear in τ, due to the linear dependence of the growth rate on the edge current density. At a density of $n=3x10^{19}m^{-3}$ (τ=0.011), the marginally stable value is increased by 35% as compared to the ideal MHD limit. At τ=0.011, the critical the pressure gradient is limited by an n=10-15 ballooning mode at a pressure gradient which is about 30% higher than the n=∞ ideal MHD ballooning limit. For the ballooning limit for each individual toroidal mode number, the increase of the marginally stable pressure gradient scales quadratically in τ. However, considering all n gives a more linear dependence because the most unstable mode number goes down with increasing τ (see Fig.3). Thus, both the kink and ballooning limits in the edge pedestal will have a significant density dependence due to stabilisation by the ion-diamagnetic drift.

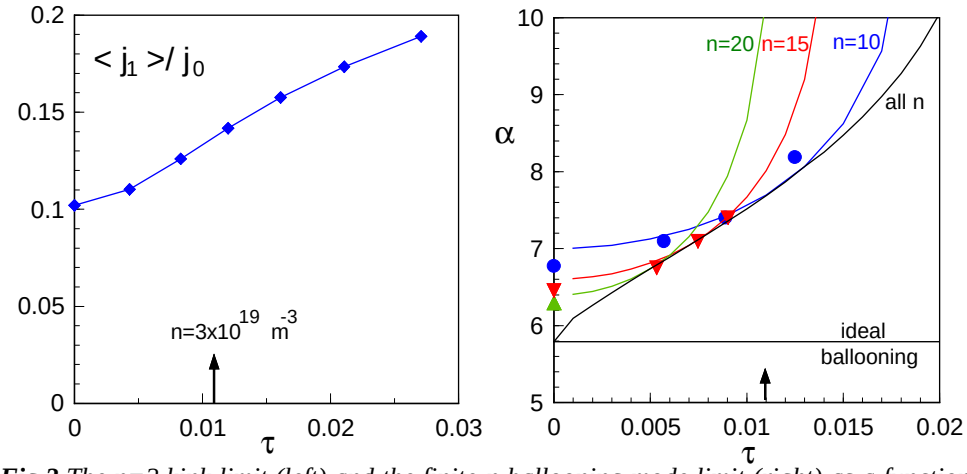

Fig.3 *The n=2 kink limit (left) and the finite-n ballooning mode limit (right) as a function of τ for JET hot-ion H-mode discharge #42677. (The marginally stable α's from MISHKA are indicated by the symbols, the curves show the values based in the ideal MHD growth rates.)*

Stability limit in Optimised Shear scenarios

The main limitation in Optimised Shear scenarios is due to the *n=1* global pressure driven kink mode [4]. The behaviour of this mode as a function of ω* does not follow the simple dispersion relation of (6). Instead, the mode does not completely stabilise for any value of ω* and the frequency of the mode has a maximum as a function of ω* (see Fig.4). This change in behaviour is related the large variation of ω* at the different rational surfaces (due to the large pressure gradients at or inside the transport barrier). One consequence is that the marginally stable mode has no frequency. Complete stabilisation can, in principle, be obtained when the density profile balances the radial change in the pressure gradient such that ω* is relatively constant as a function of radius (see Fig.4). However, based on the ideal MHD growth rates, $\lambda^2 \sim (\beta_p - \beta_{pm})$, the increase in the marginally stable beta would scale only quadratically with τ. The influence on the ion drift velocity on the n=1 stability limit in JET OS discharges is therefore very small.

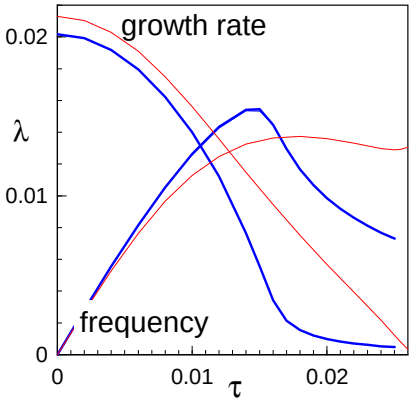

Fig. 4 *The growth rate and frequency of the n=1 mode as a function of τ with a large radial variation of ω* (full lines, blue). Also shown (thin lines, red) is a case with a small variation in ω*.*

Conclusions

The MISHKA MHD stability code has been extended to include, self-consistently, the ion-diamagnetic drift velocity. Both the kink and the finite-n ballooning limit in the edge pedestal show significant stabilisation due to the ion drift. As a consequence, the edge stability limits depend on the density, being more stable at low density. Also, the most unstable ballooning mode has a medium-n toroidal mode number which decreases with density, the width of the mode is of the order of the width of the edge pedestal. This gives a more consistent picture for the interpretation of ELMs being due to the medium-n ballooning modes, as compared to strongly localised n→∞ ideal MHD ballooning modes which are expected to lead to small-scale turbulence instead of the discrete ELM events. The stabilising influence of the ion drift velocity is much less important for the global pressure driven modes relevant in the Optimised Shear scenarios.

Acknowledgement V.V. Parail and G. Corrigan are gratefully acknowledged for the JETTO results.

References

[1] A.B. Mikhailovskii et al., Plasma Phys. Rep. **23** (1997) p.844.
[2] A.B. Mikhailovskii, Plasma Phys. Control. Fusion, **40** (1998) p.1907.
[3] J.W. Connor et al., Phys. Plasmas, Vol.5, No.7 (1998) p.2687.
[4] G.T.A. Huysmans et al., Nuc. Fusion, Vo.39 No.11, (1999) p. 1489.